# AUTOMATED TRACKING AND MODELING OF MICROTUBULE DYNAMICS

*M. Saban*[1], *A. Altinok*[2], *A. Peck*[3], *C. Kenney*[1], *S. Feinstein*[3], *L. Wilson*[3], *K. Rose*[1], *B. S. Manjunath* [1]

Center for Bio-image Informatics
Dept. of Electrical and Computer Engineering[1], Dept. of Computer Science[2],
Dept. of Molecular, Cellular and Developmental Biology[3]
University of California Santa Barbara, Santa Barbara, CA 93106
website: http://www.bioimage.ucsb.edu

## ABSTRACT

The method of microtubule tracking and dynamics analysis, presented here, improves upon the current means of manual and automated quantification of microtubule behavior. Key contributions are increasing accuracy and data volume, eliminating user bias and providing advanced analysis tools for the discovery of temporal patterns in cellular processes. By tracking the entire length of each resolvable microtubule, as opposed to only the tip, it is possible to boost dynamics studies with positional information that is virtually impossible to collect manually. We demonstrate the method on the analysis of a microtubule dataset, which was manually tracked and analyzed in the study of $\beta$III-tubulin isoform. Our results show that automated recognition of temporal patterns in cellular processes offers a highly promising potential.

## 1. INTRODUCTION

Microtubules (MTs) are highly dynamic cylindrical structures in the cytoskeleton, consisting of $\alpha$ and $\beta$ tubulin proteins [1]. Their role in cell division is especially important since a misregulation of their dynamic behavior causes chromosome mis-segregation and is associated with cancerous cell growth. Owing to their importance for cell cycle and basal function, current research groups study MTs in terms of structure, localization and dynamic behavior under different experimental conditions such as drug treatment, incubation with MT associated proteins and/or tubulin isoforms [2]. Possible regulatory mechanisms orchestrating MT activity and the mechanics of such activity in particular are important discoveries in the way of understanding how cells work. To that end, researchers acquire MT videos using time-lapse fluorescence microscopy and quantify growth and shortening characteristics.

Typically, data is collected (tracking 3-6 MT tips per video) and analyzed manually to arrive at statistical conclusions. Problems with the current method are $i$) limited sample sizes, $ii$) bias and variability in human judgement such as tracking more active MTs, and $iii$) rough estimates of MT lengths. In this work, we present a system addressing these problems by automating the MT tracking task. Furthermore, with the increase in track volume we are able to model MT dynamics using machine learning techniques. In the process, substantially more data become available to examine specifics of activity that is practically impossible to handle manually. Our results agree with manually established conclusions and, additionally, we illustrate the usefulness of computational models to gain further insights in regulatory mechanisms.

The paper is organized as follows. Section 2 reviews the related work. Section 3 presents the tracking approach. Section 4 presents the modeling of MT behavior. Section 5 gives experimental results of the proposed method. Biological significance and conclusions are discussed in Section 6.

## 2. PREVIOUS WORK

In the literature few papers [3–7] have addressed the MT detection and tracking problems. We are not aware of any published work that attempts to model MT behavior using machine learning techniques. In [5], the authors propose an automated approach to extract the MT plus-end with a coarse to fine scale scheme consisting of volume enhancement and plus-end segmentation. In [6], the MTs are extracted in terms of consecutive segments by solving Hamilton-Jacobi equations. In [4], an initial point is selected on a MT and the procedure generates a stack of points representing the MT using tangent constraints. Once the MT is detected, it is tracked in time while constraining the search space in a normal direction around MT points. The work in [7] presents a framework for detecting and tracking diffraction images of linear structures in differential interference contrast (DIC) microscopy. The method requires the user to select few points on the MT, dividing it into segments. Recent techniques utilize speckle microscopy to track fluorescent tags [8], however due to the probabilistic nature of tagging, MT tips may or may not consist of tagged molecules.

This study was funded by Center for Bioimage Informatics under grant NSF-ITR 0331697.

## 3. AUTOMATED MICROTUBULE TRACKING

We propose a tracking procedure consisting of three conceptual parts, $i$) tip detection in the first frame, $ii$) tracking tip position in subsequent frames, and $iii$) extracting MT bodies.

### 3.1. Tip detection in a video frame

Given an initial video frame, we detect all MT tips by filtering. A second derivative of Gaussian kernel matched to image locations at different orientations reveals dark curvilinear structures on light background. Let the intensity function in the window of interest $W$ be denoted as $I_W$, the output after filtering the window is as follows:

$$I^f_W(x,y) = \max_{\theta}(I_W(x,y) * G''_{\sigma,\theta}(x,y)) \qquad (1)$$

where $G''_{\sigma,\theta}(x,y)$ is a second derivative Gaussian kernel with scale $\sigma$, taken along a direction $\theta$. A value of 2 for $\sigma$ is chosen experimentally based on the MT width. Example of filtering is shown in Fig. 3.b.

A binarized mask is then computed showing the locations of MT polymer. The mask is thinned leaving one-pixel wide representations of each MT body. Next, the line endings are found on thin MTs by morphological processing. An example of MT tip detection is shown in Fig. 1.

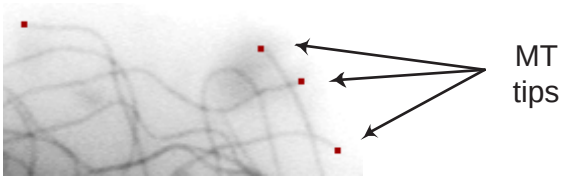


**Fig. 1**. An example of tip detection in a window.

### 3.2. Tracking tip position

After detecting MT tips in the initial frame, we proceed to track each tip separately by searching for the closest match in subsequent frames. The input to the tip tracking algorithm at time $t$ is the tip position $tip_{t-1}$ at time $t-1$ and a search window around it. Within the search window, the tracking algorithm locates best matching tip ($tip_t$) using constraints on tip motion and MT curvature.

### 3.3. Active Contour-based formation of the MT body

Computing MT dynamic parameters from the tip locations results in inaccurate lengths when the MT shape is not linear. Moreover, MTs move laterally or change shape from frame to frame which affect the calculated length in the case of following tips. For instance, manual methods compute the lengths in frames by taking the Euclidean distance between tip location and an arbitrarily selected reference point on MT body, which are then used to find the growth or shortening values in consequent frames.

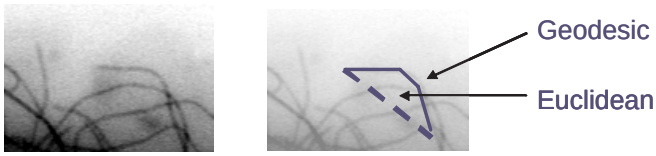


(a) (b)

**Fig. 2**. Estimate of length (a) original, (b) Euclidean vs geodesic.

Instead, computing the length along the body (i.e. a geodesic) is a more accurate alternative, as in Fig. 2. Beside accurate length computation, tracking the MT body enables further insights, e.g. populations of MTs can be positionally tracked over time reflecting possible macro-trends in tubulin polymer placement in the cell periphery.

We proceed to compute the MT body in the first frame as shown in Fig.3. Note that we consider the ending point on the MT to be fixed along the MT track for the remaining frames. For subsequent frames, the problem of extracting the MT body is performed by deforming an active contour between the fixed ending point and the tracked tip in every frame. The active contour is based on line features and curve smoothness constraints. Example tracking results are shown in Fig. 4.

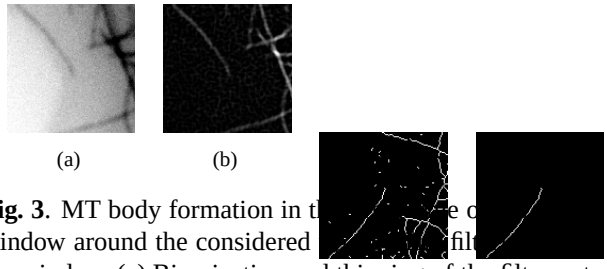

(a) (b)

**Fig. 3**. MT body formation in t e o A window around the considered fil of the window, (c) Binarization and thinning of the filter output, (d) The extracted MT body based on the point with largest Euclidean distance to the tip.

## 4. MODELING MICROTUBULE BEHAVIOR

Traditional analysis of MT dynamics consists of comparing statistics of dynamics parameters for different conditions. We propose a complementary measure whereby MT activity is modeled by Hidden Markov Models (HMM) per experimental condition. HMMs have been successfully used in modeling speech [9] and other activity, and possess interpretable model properties. HMMs are probabilistic generative models capturing statistics of a process from observation sequences (generated by the process) in *hidden* states. For example, if tracks of MTs are the observation sequences, captured statistics may be indicative of certain cellular processes causing the

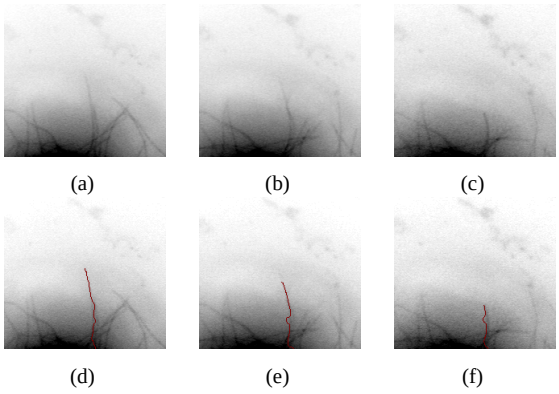

**Fig. 4**. Example frames from automatically computed MT tracks. Originals (a,b,c) and respective tracks (d,e,f). The tracked MT exhibits shortening in this case (picture best seen on the pdf version)

observed activity. Concisely, HMMs are described by parameters $\lambda = (\pi, \mathbf{A}, \mathbf{B})$, where $\pi_i$ are prior, $a_{ij} \in \mathbf{A}$ are transition, and $b_{ij} \in \mathbf{B}$ are emission probabilities.

### 4.1. Application of HMMs to microtubule dynamics

The premise of HMMs is that given MT tracks as observations $T$ for a condition (e.g., $\beta$III-Taxol©), we can find a model $\lambda$ such that $P(\lambda|T)$ is maximum. Then, we can evaluate the probability that a track $r$ is generated by the model $\lambda$ by calculating $P(r|\lambda)$. Essentially, $P(r|\lambda)$ is a probabilistic measure of association between the typical behavior modeled by $\lambda$ and the observed track $r$. Finding a $\lambda$ for each experimental condition makes it possible to (probabilistically) quantify similarities in conditions. Furthermore, parameters of each model can be examined to assess the behavioral characteristics of MTs, such as the probabilities of transitions between the different states of growth and shortening. Finally, most likely state sequences generating observed tracks can be examined to evaluate possible changes in regulatory mechanisms.

## 5. EXPERIMENTS AND RESULTS

A generally established finding is that Taxol© inhibits MT dynamics. In this work, we tracked MTs in videos from [2]. A total of 330 tracks were extracted after a visual inspection of the tracking results. Five conditions were recorded, $\beta$III-tubulin, $\beta$III-Taxol©, $\beta$III-Taxol© uninduced, $\beta$I-tubulin, and $\beta$I-Taxol© denoted by $\{\beta III, \beta IIIt, \beta IIItu, \beta I, \beta It\}$. The study analyzes the potential for Taxol© resistance conferred by tubulin isoforms. Results in [2] show that two groups of conditions have similar dynamics: $\{\beta III, \beta IIIt, \beta I\}$ and $\{\beta IIItu, \beta It\}$.

We train a separate HMM for each of the classes. To avoid over-fitting, we use the technique of cross-validation for model selection [10]. We experimented with models having 3 to 5 states with both left-to-right and fully-connected topologies and using a 4-fold cross-validation.

| | $\beta III$ | $\beta IIIt$ | $\beta IIItu$ | $\beta I$ | $\beta It$ |
|---|---|---|---|---|---|
| $\beta III$ | 0 | 0.068 | 0.066 | 0.029 | 0.065 |
| $\beta IIIt$ | 0.068 | 0 | 0.080 | 0.064 | 0.090 |
| $\beta IIItu$ | 0.066 | 0.080 | 0 | 0.076 | 0.049 |
| $\beta I$ | 0.029 | 0.064 | 0.076 | 0 | 0.070 |
| $\beta It$ | 0.065 | 0.090 | 0.049 | 0.070 | 0 |

**Table 1**. Dissimilarities between the HMMs of different experimental conditions in the $\beta$-III study [2].

### 5.1. Quantifying similarities between experimental conditions

Similarities between different experimental conditions have thus been established for a number of test subjects, yet primarily in a qualitative manner. We use the constructed HMMs to estimate a quantitative dissimilarity measure between the different experimental conditions. The method of comparing two HMMs is based on the technique discussed in [9]. Consider we have two HMMs with parameters $\lambda_1$ and $\lambda_2$. The following measure can be used to find the distance (dissimilarity) between $\lambda_1$ and $\lambda_2$:

$$D(\lambda_1, \lambda_2) = \frac{1}{T_1}\left(\log P(O^{(2)}|\lambda_1) - \log P(O^{(2)}|\lambda_2)\right) \quad (2)$$

This dissimilarity measure quantifies how the observations $O^{(2)}$ match $\lambda_1$ versus matching its own model $\lambda_2$. We use a symmetric version of the measure in (2). We show in Table 1 a five by five matrix showing the distances between pairs of HMMs describing the five experimental conditions in the $\beta$ tubulin isotype study [2]. The smaller the distance, the more similar are the two experimental conditions. Investigating the second row in Table 1, we directly conclude from the distance between the $\beta$-III + Taxol and $\beta$-III and the distance between $\beta$-III + Taxol and $\beta$-I + Taxol that Taxol does not have the same suppressing effect on cells over-expressing the $\beta$-III tubulin protein as $\beta$-I.

An alternative method to visualize the distances between the five experimental conditions is to embed the distance matrix in Table 1 into a two dimensional space using multi-dimensional scaling (MDS) [11]. The resulting two dimensional space is shown in Fig. 5. Visually, the two groups of dynamics can be separated as shown by the two ellipses on the figure. However, we observe that the $\beta$-III + Taxol condition is farther from the $\beta$-III and $\beta$-I conditions, which suggests that, though that all three conditions are characterized by high dynamics, they are not all equidistant in terms of behavior.

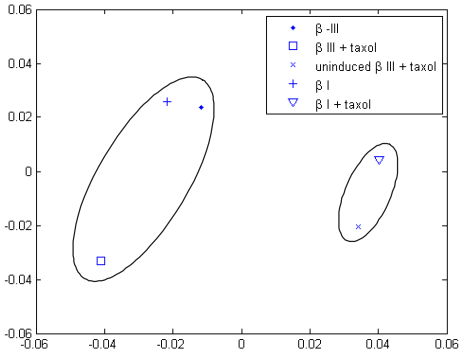


**Fig. 5**. A two-dimensional embedding of the distances in Table 1. The two ellipses represent the two group of dynamics $g_1 = \{\beta III, \beta IIIt, \beta I\}$ and $g_2 = \{\beta IIItu, \beta It\}$.

## 6. BIOLOGICAL SIGNIFICANCE AND CONCLUSIONS

In this work, we present an automated system for MT dynamics research [12]. Our method arrives at similar biological conclusions in a fraction of time required by manual methods. Automated tracking increases dynamics data volume significantly with high accuracy. Furthermore, it eliminates user bias and enables standardization of tracking across MT research labs. On the tracking side, a significant benefit of tracking the full body as opposed to the tip alone, is that movement of MT populations can be tracked over time, reflecting reorganization of tubulin polymer in the cell periphery. Such insights would be extremely valuable in the study of gross cytoskeletal rearrangements during cytokinesis, intra/intercellular signaling, cell division, and morphological development.

On the analysis side, probabilistic models describing typical activity can be used in detecting patterns, establishing behavioral MT populations which are potentially subject to common regulatory influences. We can address questions of commonalities between regulatory mechanisms influencing MT behavior, be they drugs or MAPs, in an attempt to establish *typical* MT behaviors under discrete conditions. Complex behavioral models based on automated tracking data may facilitate the union of previously isolated cell-autonomous (MAPs) and pharmacological study datasets, furthering our understanding of regulatory mechanisms of MTs that serve as both therapeutic targets (cancer) and agents of pathology (AD, FTDP-17). Our method preserves intact MT *life-histories* or event sequences, recording the context before and after each dynamic event. We are no longer limited to the analysis of individual events as the sole unit of dynamics. We believe that by considering an entire life history as a unit of MT dynamics, we will gain a new insight in establishing behavioral distributions.

We are investigating possible trends in neighborhood relationships among MTs, which could stimulate novel biological studies. Looking beyond the traditional dynamics parameters should be feasible with modification to the proposed method. Such parameters, such as spatial patterns of MT populations, are manually infeasible features to be computed. Slight modifications to our method will allow us to look beyond the traditional dynamics parameters and elucidate higher-level processes such as spatial trends in MT polymer and behavioral transitions in response to changing conditions.

## 7. REFERENCES

[1] Bruce Alberts et al., *Molecular Biology of the Cell*, Garland Science, 4th edition, 2002.

[2] K. Kamath et al., "$\beta$iii-tubulin induces paclitaxel resistance in association with reduced effects on microtubule dynamic instability," *J. Biol. Chem.*, vol. 280, no. 13, pp. 12902–12907, Apr 2005.

[3] L. Liang et al., "Extraction of 3d microtubules axes from cellular electron tomography images," in *Proc. of ICPR*, 2002, vol. 1, pp. 804–807.

[4] S. Hadjidemetriou et al., "Automatic quantification of microtubule dynamics," in *Proc. of Int. Symp. on Biomedical Imaging: From Nano to Macro*, 2004.

[5] Ming Jiang, Qiang Ji, and Bruce F. McEwen, "Automated extraction of microtubules and their plus-ends," in *WACV/MOTION 2005*, 2005, pp. 336–341.

[6] S. Hadjidemetriou et al., "Segmentation and 3d reconstruction of microtubules in total internal reflection fluorescence microscopy (tirfm)," in *MICCAI*, 2005.

[7] G. Danuser et al., "Tracking differential interference contrast diffraction line images with nanometre sensitivity," *Journal of Microscopy, 198*, pp. 34–53.

[8] P. Vallotton et al., "Tracking retrograde flow in keratocytes: News from the front.," *Molecular Cell Biology*, vol. 16, pp. 1223–1231.

[9] L. Rabiner and B. H. Juang, *Fundamentals of Speech Recognition*, Prentice-Hall, 1993.

[10] Vladimir S. Cherkassky and Filip Mulier, *Learning from Data: Concepts, Theory, and Methods*, John Wiley & Sons, Inc., 1st edition edition, 1998.

[11] I. Borgand and J.Lingoes, *Multidimensional similarity structure analysis*, Springer-Verlag Inc., New York, NY, 1987.

[12] Arshad Desai et al., "Microtubule polymerization dynamics," *Annual Review of Cell and Developmental Biology*, vol. 13, pp. 2720–2728, November 1997.